The VERT-X calibration facility: development of the most critical parts.

A. Moretti[a], G. Pareschi[a], S. Basso[a], D. Spiga[a], M. Ghigo[a], G. Sironi[a], G. Tagliaferri[a], M. Civitani[a], V. Cotroneo[a], N. La Palombara[b], M. Uslenghi[b], M.Tordi[c], S. Delorenzi[c], F. Dury[c], G. Valsecchi[d], F. Zocchi[d], F. Marioni[d], D. Vernani[d], F. Amisano[e], G. Parissenti[e], G. Parodi[f], M. Ottolini[f], P. Corradi[g], M. Bavdaz[g], and I. Ferreira[g]

[a]INAF-Brera, via Brera 28, 20123 Milan, Italy
[b]INAF-IASF, via Corti 12, 20133 Milan, Italy
[c]EIE, Via Torino, 151 A 30172 Mestre (VE), Italy
[d]Media Lario, Via al Pascolo, 23842 Bosisio Parini (LC), Italy
[e]GP Advanced Projects, Via Tartaglia 14, 25064 Gussago (BS), Italy
[f]BCV Progetti, via Sant'Orsola 1, 20123 Milan, Italy
[g]ESA-ESTEC, Keplerlaan 1, 2201 AZ Noordwjik, The Netherlands

ABSTRACT

The ATHENA X-ray telescope will be the largest X-ray optics ever built. The ground calibration of the mirror assembly raises significant difficulties due to its unprecedented size, mass and focal length. The VERT-X project aims at developing an innovative calibration facility which will be able to accomplish to this extremely challenging task. The design is based on an X-ray parallel beam produced by a source positioned in the focus of a highly performing X-ray collimator; the 6 cm-beam will be accurately moved by a raster-scan mechanism covering all the ATHENA optics. The main driving factor in the VERT-X design is the ATHENA calibration requirement on the accuracy in the HEW measure. The VERT-X project, started in January 2018, is financed by ESA and conducted by a consortium that includes INAF together with EIE, Media Lario, BCV Progetti and GPAP. In this paper we describe the first phases of the development of the most critical parts of the system, namely the raster-scan vertical tube, tip-tilt metrology, first translation axis together with the X-ray source - collimator system. These parts will be the core of the VERT-X testing system: the functioning of the whole system critically depends on their performance.

Keywords: Astronomy, X-ray, optics, ATHENA, calibration, facility

1. INTRODUCTION

The Advanced Telescope for High Energy Astrophysics (ATHENA) is the second Large mission of the ESA Cosmic Vision Science program, selected in 2014 to address "The Hot and Energetic Universe" science theme.[1] ATHENA mission project successfully concluded the feasibility study (phase A) in November 2019 and is currently working to the preliminary definition (phase B1). The Mission Adoption Review is scheduled in 2022, with the the adoption of the mission in the ESA Science Program expected by the end of that year. The launch is foreseen for the early 2030s.[2]

ATHENA will represent a powerful X-ray observatory for all astrophysics fields: the ambition of the mission will be the study of the Universe hot baryonic components, from super massive black holes (SMBH) in the center of galaxies in the early Universe to galaxy clusters and their large structures.

These goals will be achieved through the largest ever built X-ray mirror which will focus 0.2-12.0 keV photons on two detectors, for spatially resolved high resolution spectroscopy (the X-ray Integral Field Unit, X-IFU) and for wide field imaging and low resolution spectroscopy (the Wide Field Imager, WFI) respectively. The mirror will be built using the ESA Silicon Pore Optics (SPO) technology which provides large effective area with excellent

Optics for EUV, X-Ray, and Gamma-Ray Astronomy X, edited by Stephen L. O'Dell, Jessica A. Gaskin, Giovanni Pareschi, Proc. of SPIE Vol. 11822, 118220K · © 2021 SPIE · CCC code: 0277-786X/21/$21 · doi: 10.1117/12.2593670

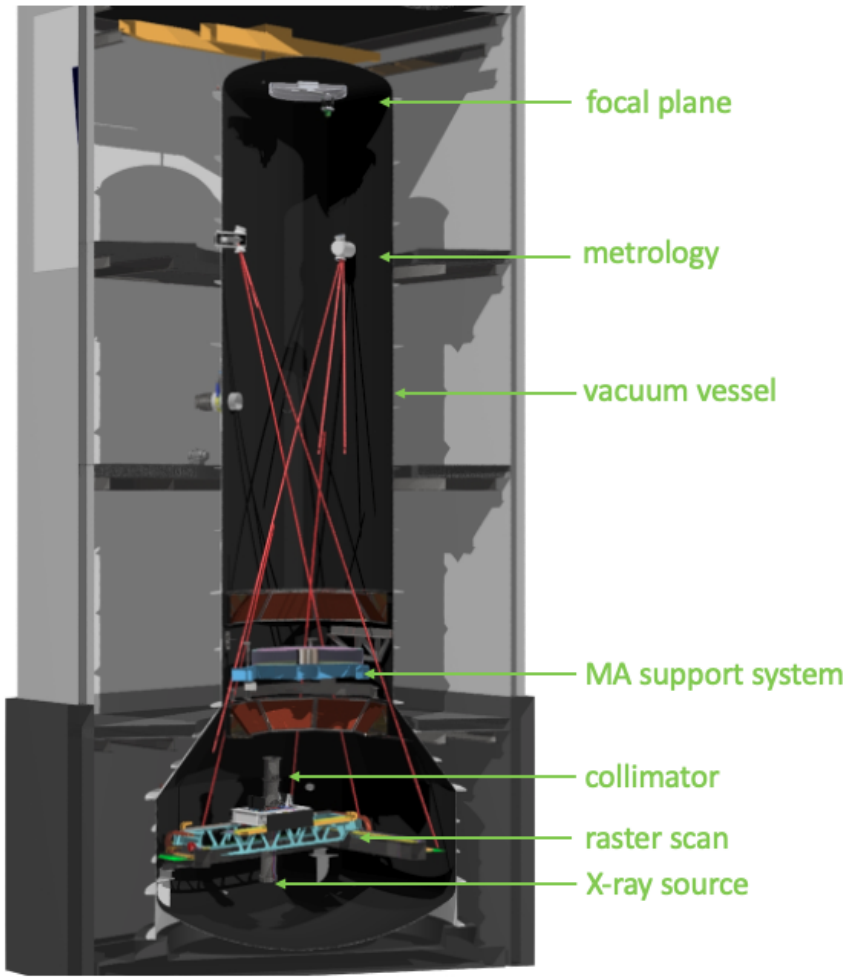

Figure 1. Design of the whole VERT-X facility, with the main parts in evidence.

angular resolution.[3] While testing and integration procedures of the single mirror modules (MM) have been well established[4,5] , the verification and calibration of the entire MA are particularly challenging and different options are still under scrutiny. In fact, to ensure that the uncertainties due to the divergence of the beam are compatible with the accuracy requirements of the calibrations, the source should be positioned at a minimum distance of 300 meters.[6] Since the largest X-ray calibration facility in Europe is the MPE Panter Lab, with a 120 m tube, this requirement could be satisfied only by a new X-ray long beam facility[7] or by a significant upgrade of the NASA X-ray & Cryogenic Facility (XRCF, https://optics.msfc.nasa.gov/).

In this context we proposed the concept of the VERTical X-ray raster-scan facility for ATHENA calibration (VERT-X). The VERT-X concept is based on the idea of producing a parallel beam positioning a point-like source in the focus of an X-ray collimator.[8] This concept is not novel and it has been already used in the BEATRIX facility[4] to test single mirror modules.

Since, for evident construction reasons, the beam amplitude has to be much smaller than the ATHENA mirror, the source-collimator system is thought to be moved by a raster-scan mechanism which covers all the optics to be calibrated. This results in the design of a calibration facility much smaller in size (as shown in Fig.1) with respect to the traditional long tube. The system is enclosed in a 20 meter high cylindrical vacuum chamber,

Send correspondence to A.M.
A.M.: E-mail: alberto.moretti@inaf.it

with the focal-plan on the top. The ATHENA MA will be positioned at the ground level. The raster-scan mechanism is positioned below that, at $\sim$ 5 m underground , completely enclosed in the vacuum chamber, with the purposes of translating and rotating the vertical tube on which X-ray source and the beam collimator are mounted.

VERT-X has many different aspects from a traditional long-tube calibration facility design. First, in principle, can produce a beam with such a low divergence which is far beyond the capabilities of long tube laboratories. Moreover, the VERT-X design compactness comes with important benefits beside the smaller amount of involved resources: the vertical geometry which largely simplifies the mirror support and reduces to zero the PSF degradation due to the lateral (perpendicular to optical axis) gravity; the small size of the beam allows to characterise the contribution of the single modules to the over-all mirror performance; finally the location of the facility can be chosen flexibly, according to the project needs. Indeed, the project is to build the VERT-X facility in the building of the Media Lario company, in continuity with the ATHENA MA integration facility.[5] This, of course, would make the direct verification of the performance of the assembled optics much easier during the integration phase.

The VERT-X project was kicked off on January 2019 with an ESA-INAF 18-month contract with the goal of producing a detailed design of the entire facility. The first output of this activity has been presented in.[9] This activity was successfully concluded in July 2020. In November 2020 a new contract was issued, with the goal of developing those that in the previous phase have been evaluated as the most critical parts of the whole system. The final aim of this 18-month activity, is to test the real performance of this innovative measuring system.

2. THE HEW ERROR BUDGET AND THE CRITICAL PARTS

According to the ATHENA Calibration plan, an absolute knowledge error (AKE) of 0.1" at 68% confidence is required for the MA HEW at all energies in te 0.3-12.0 KeV energy band all over the field of view.[6] This has been the main driving factor in the VERT-X design.

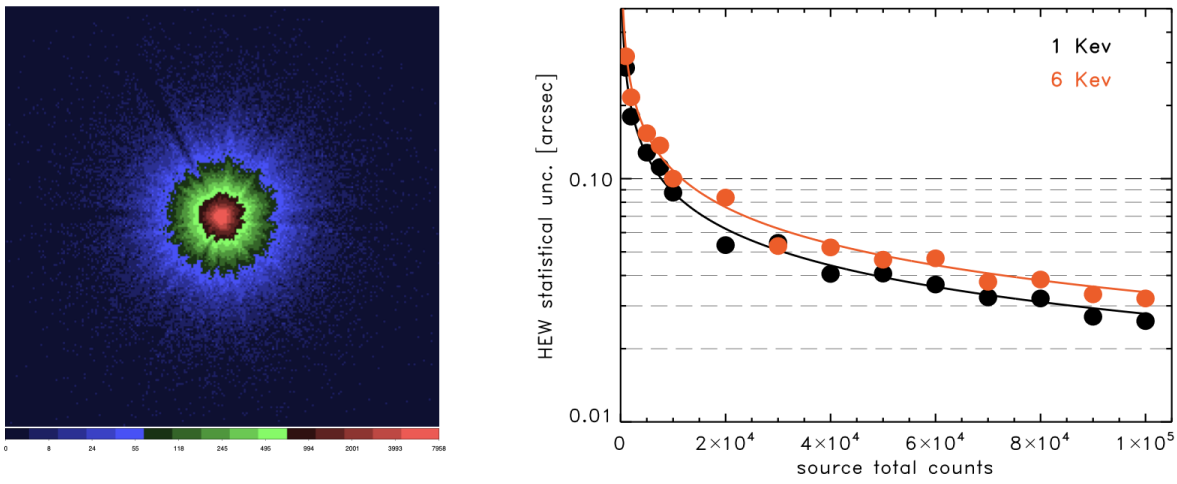

Figure 2. The simulated ATHENA PSF (left panel), assumed to calculate the statistical uncertainty on the HEW measure, as function of the accumulated events (right panel).

The PSF observed at VERT-X, $\mathrm{PSF_{VTX}}$, will be given by the convolution of the ATHENA MA intrinsic PSF $\mathrm{PSF_{MA}}$, with the residual beam divergence $\mathrm{PSF_{BEAM}}$. Therefore the observed $\mathrm{HEW_{VTX}}$ will be given by

$$\mathrm{HEW^2_{VTX}} = \mathrm{HEW^2_{MA}} + \mathrm{HEW^2_{BEAM}}. \quad (1)$$

Simply from the error propagation, it follows that the uncertainty on the $\mathrm{HEW_{MA}}$, which is the goal of verification/calibration, will be given by

$$\sigma^2_{\mathrm{MA}} = \frac{\mathrm{HEW^2_{VTX}}}{\mathrm{HEW^2_{MA}}}\sigma^2_{\mathrm{VTX}} + \frac{\mathrm{HEW^2_{BEAM}}}{\mathrm{HEW^2_{MA}}}\sigma^2_{\mathrm{BEAM}}. \quad (2)$$

The first term of the quadratic sum (σ^2_{VTX}) is the statistical error, the second the systematic (σ^2_{VTX}). Note that both the errors are weighted by the ratio with the intrinsic $\mathrm{HEW_{MA}}$.

2.1 The statistical error

For a given PSF, the statistical error on the HEW measure directly depends on the (square root of) the accumulated photons. In order to estimate the expected statistical error on the HEW of the ATHENA MA as measured at the VERT-X facility, we started from the ray-tracing output[10] showed in Fig.2: this has been produced with $1.5\times\ 10^6$events at 1 keV energy on axis and contains a full treatment of error terms: (i) in-plane and out-of-plane figure errors/response focal length/kink angle errors; (ii) reflection coating and surface roughness/scattering parameters; (iii) translational integration errors; (iv) rotational integration errors. As said, the PSF model allows us to estimate the expected statistical error in the HEW calibration as function of the number of photons collected during the calibration tests. To this aim, starting from the best fit model of the ray-racing PSF we simulated PSF with different numbers of photons, ranging from 1000 to 100,000. At a given number of collected events we simulated 100 times PSF and measured the HEW. In Fig. 2, for each number of photons, we report the standard deviation of the 100 measures. As expected, the HEW measure accuracy follows the number of counts with a slope of 0.5. We find that, to keep the statistical uncertainty at the level of 0.05", corresponding to 50% of the total HEW error budget, ∼40,000 counts per energy bin are required. This statistical level is compatible with the VERT-X concept of operation with the main factor being the detector sustainable rate[9] .

2.2 The systematic error

The systematic term in the error budget, which is the beam divergence, is caused by several independent contributions. In the design phase (i) the source dimension $\mathrm{HEW_{SOU}}$, (ii) the mirror error $\mathrm{HEW_{MIR}}$, (iii) the raster-scan tracking uncertainty $\mathrm{HEW_{TRK}}$ and (iv) the relative heat-induced displacement between source and collimator $\mathrm{HEW_{THR}}$, have been individuated as the major ones:[9]

$$\mathrm{HEW^2_{BEAM}} = \mathrm{HEW^2_{SOU}} + \mathrm{HEW^2_{MIR}} + \mathrm{HEW^2_{GRV}} + \mathrm{HEW^2_{PNT}}. \quad (3)$$

Therefore, the requirements on the ATHENA MA PSF calibration accuracy directly translate into requirements on these elements, which are considered the most critical part of the system and will be the subject of this article from here on out. The expected values of the single terms of the systematic error budget have been estimated at the design level and are summarised here in Tab 1.

Table 1. HEW systematic error budget estimated at the design level.

ELEMENT	VALUE	ERROR
$\mathrm{HEW_{SOU}}$	0.80"	0.16"
$\mathrm{HEW_{MIR}}$	0.75"	0.20"
$\mathrm{HEW_{TRK}}$	0.27"	0.24"
$\mathrm{HEW_{THR}}$	0.10"	0.10"

Assuming an intrinsic HEW of 5.0" for the ATHENA MA and filling the equation with the numbers here reported, we find that in the nominal operations the expected measure HEW, will be 5.2", accounting for a 0.05" statiscal error, as discussed in the previous Section. This would allow us to estimate the intrinsic $\mathrm{HEW_{MA}}$ with an error of 0.096" at 68% confidence, just within the requirement.

3. VERT-X CRITICAL ITEMS: STARTING THE DEVELOPMENT PHASE

The purposes of the current activity which is described hereafter is the developing of the elements that mostly contribute to the HEW measure systematic error budget. The final assessment of their performance will be performed by means of the laboratory measures of their contribution to the beam divergence. As described in

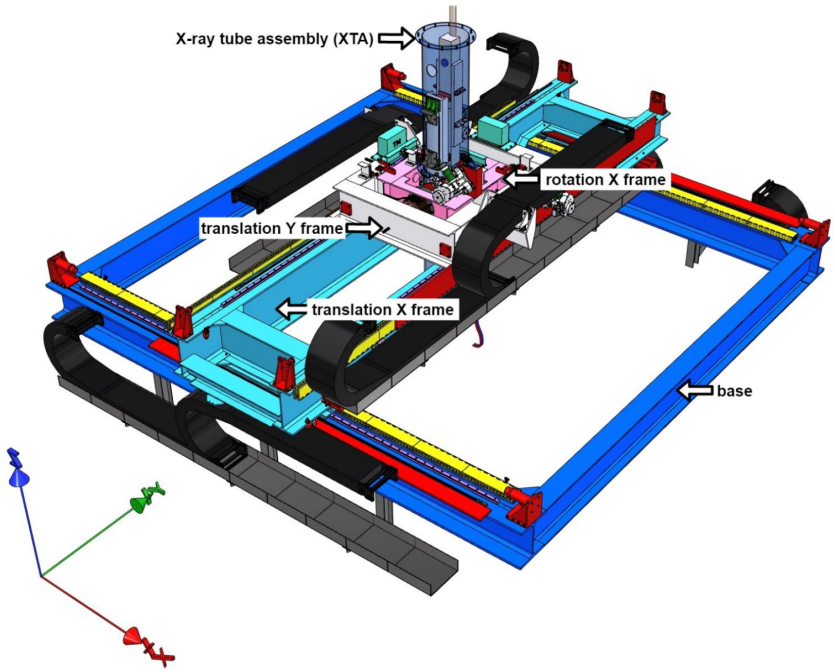

Figure 3. 3D view of the raster-scan mechanism with the main parts highlighted.

the previous Section, they are the parallelizing mirror, the X-ray source both mounted on the raster scan vertical tube, together with the raster scan X-axis rotation and Y-axis translation frames. After the development and manufacturing, raster-scan tracking error (HEW_{TRK} in the previous Section) will be accurately estimated by a test campaign together with a first assessment of the displacement induced by thermal gradient on the vertical tube. The contribution to the beam divergence produced by the source dimension (HEW_{SOU}) coupled with the collimator error (HEW_{MIR}) will be measured in X-ray at the MPE/PANTER laboratory together with the final assessment of the term due to the thermal gradient along the tube (HEW_{THR}).

3.1 The raster-scan

The raster-scan mechanism allows the collimated X-ray beam to perform four movements, two translations on the horizontal plane and two tilts around the two horizontal axes. It consists of the following main parts: the base, the X and Y-axis translation frames and the tube also called the X-ray tube assembly (XTA) (Fig.3) . All these elements are designed in the same material (AISI 304 stainless steel) in order to have the same thermal behaviour as the vessel and to ease the mechanical interface. The base is the fixed part of the system: it is linked to the thermal vacuum chamber (TVC) and supports the X-axis translation frame, which consists of a bridge joining the base sides parallel to the X-axis. The translation along the X-axis is achieved by moving the bridge on top of the base. Both the base and the X-axis translation frame have been not considered critical and their development is not included in the current activity.

3.1.1 Y-axis translation frame, the trolley

Y-axis translation frame, as indicated by its name, the first critical item, is the frame moving over the bridge (X-axis translation frame) along the Y-axis. It consists of a trolley with iron-less linear motors. The magnets

segments are installed on the two bridge beams, consequently the two motor coil segments are installed on trolley, one per side. The motor coil segment interface plates are active cooled by a water/glycol mixture. This coolant pass through a cooling unit installed directly into contact with motor and with its interface plate. As shown in the left panel of Fig. 4 the bottom part of the trolley hosts the elements in charge of the Y-axis translation. The sliders which run onto the linear guides; the coil drives which are fixed on their cooling support; the encoder head which runs over the encoder tapes and precisely locates the frame. The calliper brake pinches and the mechanical bumper which dissipates the energy of the translation to a mechanical buffer in case of collision.

On each of the raster scan four movements, fail safe parking brakes are foreseen. In normal operation they open and close the calipers only when motion is already stopped by the servo motors, so no wear and relevant particles pollution are expected. Only in emergency condition they close the calipers with relative motion. The translation X frame hosts two fail/safe brakes with electrical calipers release installed on its both extreme sides to hold the bridge in position while trolley is scanning. The translation Y frame hosts only one brake due to its small dimension. The rotation X frame and the XTA host one electromagnetic brakes each. They are situated at one side of the rotation axis.

The top part of the trolley hosts elements in charge of the rotation around the X-axis. The torque stator drive; the encoder head to precisely control the frame inclination; the limit switches which is triggered by the rotation X frame when exceeding the software movement final stop; the tiltmeters providing the real time slope (a description of the tiltmeters is reported below). the cable carrier damping assembly pulling and pushing the carrier minimizing the vibrations.

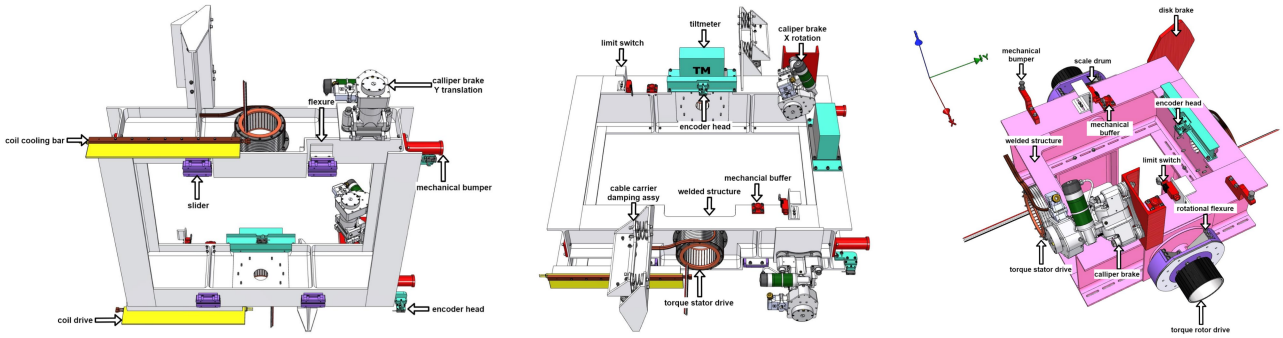

Figure 4. Y-axis translation frame (the trolley, bottom and top view respectively) and X-axis rotation frame (the Gimbal mount).

3.1.2 X-axis rotation frame, the Gimbal mount

Rotation around the X-axis is acheived by a Gimbal mount hosted by the Y-axis translation frame. In order to rotate the vertical tube, two torque motors are used, one per gimbal side. The rotors with magnets are installed on the two Gimbal shafts, consequently the two stators with motor coils are installed on the trolley, one per side. The motor stators are active cooled by a water/glycol mixture too. The X side of the Gimbal mount hosts the elements responsible for the rotation around the X-axis of the vertical tube XTA. These are the rotational flexure assuring the XTA X rotation and a constant preload for the torque drive; the torque rotor drive; the encoder scale drum read by the translation Y frame encoder head for the precise control of the X rotation; the limit switches being triggered by the XTA when exceeding the software movement final stop; Along the other direction the frame hosts the elements in charge of the rotation around the Y-axis: the torque stator; the encoder head placed over the XTA scale drum to precisely control the tube inclination;

3.1.3 The vertical X-ray tube assembly, XTA

The X-ray tube assembly is the very core of the raster-scan, hosting the two main elements: the X-ray source and the collimator. These two elements are pieced together in a stainless-steel round tube to get the best rigidity between them. The tube itself is inserted in the axis assembly and positioned in order to be well balanced with

the help of counterweights: balancing counterweights assure the COG centring along the X-Y axes, while the centering along the Z-axis is achieved moving the tube up and down. The axis assembly hosts the elements in

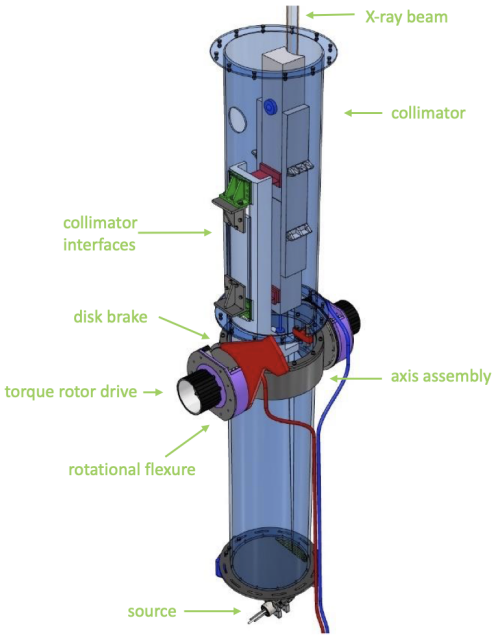

Figure 5. The 3D view of the tube design with the source and collimator in evidence.

charge of the rotation along the Y-axis. The rotational flexure which assures the XTA Y-axis rotation and a constant preload for the torque drive; the torque rotor drive; the encoder scale drum read by the rotation X frame encoder head;

3.1.4 Tip-tilt metrology and tiltmeters

A tip-tilt metrology system has been introduced in the design to measure and correct the attitude variation of the X-Y translation stages as they move across the working area. This system provides the measurement of the attitude variation, which is used by the control system to correct the pointing set-point in real-time, keeping the alignment of the X-ray beam within the required error range, so to minimize the beam divergence and consequently the raster scan contribution to the HEW measure error budget . Off-the-shelf tilt-meters based on liquid bulbs are not a suitable solution for the VERT-X raster scan, since they are subject to disturbances caused by in-plane accelerations and are characterized by a relatively large time constant. Instead we chose the systems developed for the ALMA sub-mm telescope.[11] These are servo-actuated tilt-meters, based on an inverted pendulum kept in position by means of electro-magnetic motors and a position feedback provided by capacitive sensors. Furthermore, the inverted pendulum is combined with an inertial rotor, which can rotate almost freely around its rotational axis, constrained by a very weak flexure. The inertial rotor has zero DC gain, and it is sensitive to inclinations only above its self-resonance frequency: the real advantage of using both mechanism combined, consists in the possibility to filter out the disturbances of the inverted pendulum by means of the rotor readings. This is particularly relevant for VERT-X, where we expect to continuously have micro-accelerations due to the rail roughness, servo-control imperfections, stick-slip occurring at the pads level. The tilt-meters have been operating on-board the 25 European antennas of the array since 2013, for a total of 50 tilt-meters. No failures have been reported so far.

3.1.5 Raster-scan operations

The nominal scan velocity is 30 mm/s. Since the beam size, orthogonal to the scan direction, is 60 mm (see below), to cover the ATHENA MA a the total path of $\sim$ 100 m is needed. This corresponds to $\sim$1 hr accounting

for ∼15 s of settling time at the start and end of each row. The tube can be tilted not only to cover all the field of view (radius 20'), but also to point up to 3° off-axis in order to simulate the stray-light contamination from an off-axis source. In particular, this number is sized in accordance with what expected without baffles.[12]

The main factors contributing to raster-scan tracking error are the thermal deformation due to temperature gradient along the raster scan structure, the non-repeatable runout of the trolley liner guide support system. In both these cases the metrology is expected to provide a correction leaving a residual uncertainty of 0.03". The third error source is the gimbal and tube axis torsions due to the bearing friction on one side and the motor to the other side; in order to compensate for this error the Gimbal and Tube motors were doubled in order to apply a symmetrical axis torque;

3.2 The collimator

The optical design of the X-ray collimator is based on a Wolter I configuration of about 1.1 m in length and an average grazing incidence angle of about 0.4°. The main driving requirements that led to the definition of

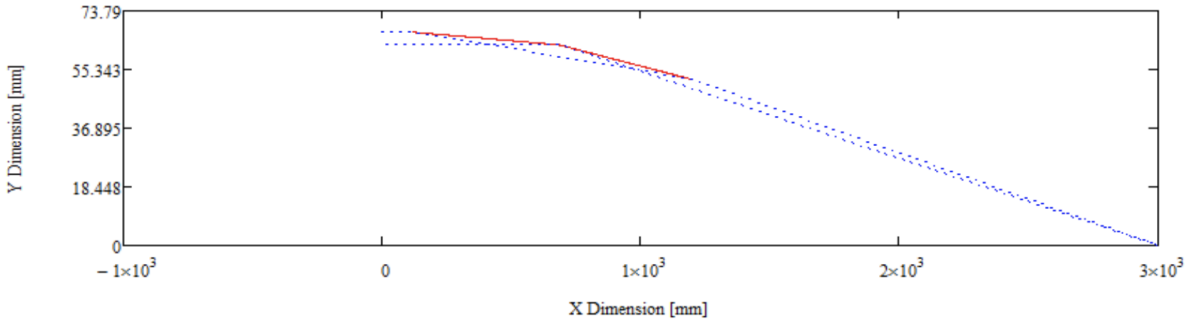

Figure 6. Optical design of the collimator.

the design are related to the needs of sufficiently high reflectivity in the spectral range between 0.2-12 keV and the limitation to $\lesssim$1" for the divergence error of the collimated beam produced by the mirror. The reflectivity requirement limits the average grazing incidence angle to less than 0.4° (Fig 6). Moreover, since micro-focus X-ray sources have dimension limited to 10-15 μm FWHM, the divergence requirement, in turn, limits the minimum distance between the source and the optics to about $\gtrsim$ 2m.

Given the above constraints, a design, based on a Wolter I configuration, has been derived (Tab 2). An alternative possible design may consist of a section of a parabolic mirror, similar to the case of BEATRIX.[4] As discussed in[9] the Wolter design has been preferred due to the the lower collimation sensitivity to alignment and source dimension.

Table 2. Summary of the mirror optical parameters.

PARAMETER	VALUE
Min. distance of mirror from source (on axis)	1800 mm
Min. collected angle	1.56 °
Max. collected angle.	1.86°
Mirror length.	1083 mm
Efficinecy @ 0.5, 1.0 ,0.5 10.0 KeV	0.82, 0.83, 0.62,0.52
Min. radial distance of the beam from axis.	52.14 mm
Radial extension of the beam	4.06 mm

Mirror mechanical design consists of two separate sections in Zerodur®, for the parabolic and hyperbolic profiles of the Wolter collimator, respectively. This solution is preferred to the monolithic collimator approach

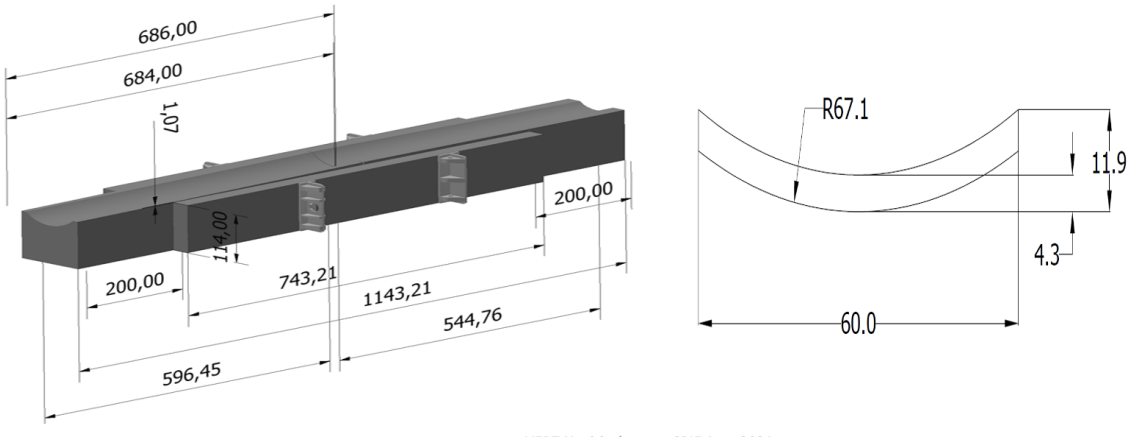

Figure 7. Mechanical design of the collimator, together with the beam footprint.

for several reasons reasons. First of all, the production of two independent shorter and lighter mirrors reduces the manufacturing and handling risks. Then, the relative alignment tolerance between the two collimator sections is loose enough to be accurately achieved by means of CMM metrology. Finally, the alignment of the parabolic and hyperbolic sections might be actively controlled either off-line (say, periodically or during calibration) or on-line (say, in real time in closed loop control).

A gap of 2 mm is present between the two sections. After alignment, the two mirror parts are held together by means of two plates of Zerodur® laterally fixed with adhesive. Alignment tolerances of the parabola to the hyperbola have also been studied investigating the impact of the displacements in the 6 degrees of freedom, 3 translational and 3 rotational (Spiga et al. in this conference).

3.3 Raster scan tube / mirror interfaces

The design of the interfaces between the raster-scan vertical tube and the mirror entailed particular attention. The point is that in case of rigid connection between mirror and the tube, even a small elongation of $\sim 10 \mu$m produced by a 1 deg temperature increase, would yield collimator deflections of 36.3 μm PtoV. This would produce a dramatic increase of the beam divergence at the level of 24.5" (HEW) . Therefore avoiding that the collimator becomes a sort of tube strengthening is mandatory. The collimator should act just a load for the tube. Collimator deformations triggered by tube deflections should result as much as possible in rigid body movements, without appreciable distortions. To achieve this result the collimator interfaces have to realize a quasi-kinematic mount, which can be obtained by proper flexures. At the bottom, the collimator axial support is aligned with collimator CG (Fig.8).

This system is expected to decouple tube and collimator structural behaviour. All interfaces connected to the collimator are designed in Invar to reduce CTE mismatch of the components rigidly connected to the collimator. In order to reduce the impact of flexures quasi-kinematic collimator mount on the tube design and to simplify the collimator integration procedure, an intermediate structure level, between collimator and tube has been foreseen. This is an L-shaped structure which allows to manipulate the interfaces in a more comfortable way (Fig.8). Moreover the presence of an intermediate interface significantly reduces the time needed for the mirror-tube integration, with important programatic benefits. The cost of this additional interface is the mass increase.

As already said, the final goal of the present activity will be the test of the source+mirror system performance in vacuum. Due to the lack of laboratories equipped to carry out tests in a vertical position, this will be performed in horizontal, differently from the nominal working configuration. Lateral gravity distortions during this test test are mitigated by an actuator force. The tube will have a hole for the actuator pusher passing. Actuator force will be adjustable around the nominal value obtained from numerical assessment, for a fine tuning on site during optical tests.

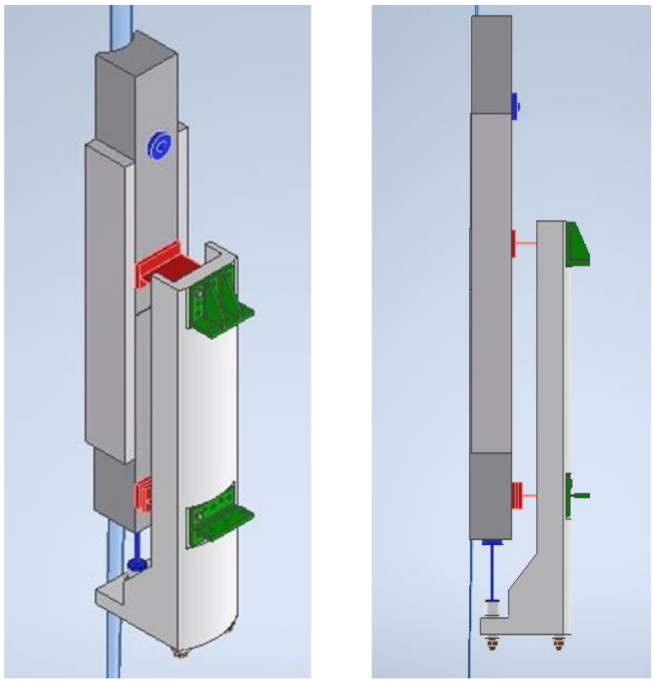

Figure 8. The X-ray source assembled on the XYZ stage

Collimator integration in vertical position appears to be the most suitable solution. An integration with horizontal collimator would need at least one force actuator to mitigate the lateral gravity distortions. Vertical integration also avoids any flexure spring back during operation, since integration and operative configurations are almost the same. Very fine alignment between tube and collimator axis is not needed since small residual misalignment can be compensated by the tube verticality setting.

3.4 The X-ray source

In the VERT-X design the X-ray source requires particular attention. Different from the standard, the VERT-X source is required to have very small size (micro-focus) and, at the same time, it has to fully operate in vacuum, which means the need of a liquid-based cooling system. Moreover, the system must not cause vibrations on the raster-scan mechanism and this can only be achieved by an ion-pump. These non-standard characteristics are provided by the SIGRAY FAAST source, a micro-focus sealed tube with a diverging beam refocus by a double parabolic mirror in order to minimize the apparent source size. With respect to the standard product, the source is provided with a customized Be window, 25μm thick, in order to extend the energy band down to values lower than 1 KeV. The source brightness profile at the exit of the double-parabolic mirror is expected to be Gaussian with a FWHM of 8 μm, as best effort. This corresponds to a divergence of the beam the order of 0.7", when positioned in the mirror focus at 2 m distance (see previous Section).

In the integration scheme the collimator will be fastened to the tube, while the X-ray source will be movable in order to be always positioned in the collimator focus. Movement along the 3 axis will be provided by a combination of three linear stages, according the configuration shown in Fig9 .

4. SUMMARY AND CONCLUSIONS

The ground verification and calibration of the ATHENA mirror assembly raises significant difficulties due to the unprecedented size, mass and focal length. We developed the design of a new facility capable of carrying out this task. The idea is based on the production of a parallel beam through a micro-focus source and a collimator that parallels the X-ray photons. The most compelling element in the project is the requirement on the PSF

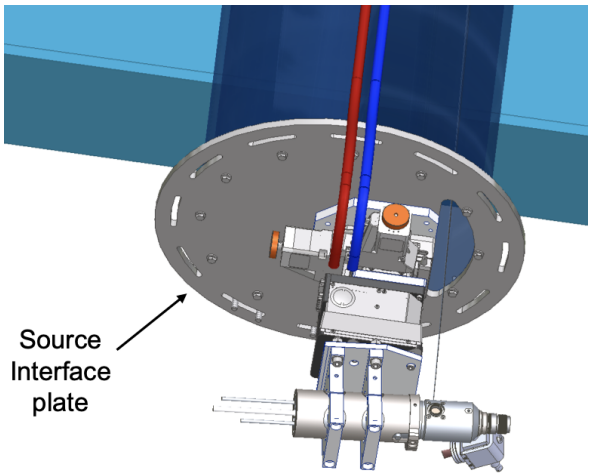

Figure 9. The X-ray source assembled on the XYZ stage

calibration accuracy. The design analysis identified the size of the source, the errors of the mirror, the raster-scan vertical tube tracking uncertainty and the relative displacement between source and mirror as the main factors in the systematic error budget of the PSF calibration. According to the preliminary assessment, at the design level, VERT-X measures will be compliant with the required accuracy with very tiny margin. In this paper we reported on the current activity of the project consortium which is the first phase of the development of the core of the VERT-X measure system: the raster scan Y-axis translation and X-axis rotation frames together with the XTA system which includes the raster-scan vertical tube, the X-ray source and the parallelizing collimator. The final goal of this activity will be the laboratory test of the real performance of the most critical parts of this innovative calibration facility.

REFERENCES

[1] Nandra, K., "The Hot and Energetic Universe: A White Paper presenting the science theme motivating the Athena+ mission," *arXiv e-prints* , arXiv:1306.2307 (June 2013).

[2] Barret, D., Decourchelle, A., Fabian, A., Guainazzi, M., Nandra, K., Smith, R., and den Herder, J.-W., "The Athena space X-ray observatory and the astrophysics of hot plasma," *Astronomische Nachrichten* **341**, 224–235 (Feb. 2020).

[3] Bavdaz, M., Wille, E., Ayre, M., Ferreira, I., Shortt, B., Fransen, S., Collon, M. J., Vacanti, G., Barrière, N., Landgraf, B., Start, R., van Baren, C., Della Monica Ferreira, D., Massahi, S., Christensen, F., Krumrey, M., Burwitz, V., Pareschi, G., Valsecchi, G., Oliver, P., Seidel, A., and Korhonen, T., "Optics developments for ATHENA," in [*Optics for EUV, X-Ray, and Gamma-Ray Astronomy IX*], *Society of Photo-Optical Instrumentation Engineers (SPIE) Conference Series* **11119**, 111190D (Sept. 2019).

[4] Salmaso, B., Basso, S., Giro, E., Spiga, D., Sironi, G., Vecchi, G., Ghigo, M., Pareschi, G., Tagliaferri, G., Uslenghi, M., Fiorini, M., Paoletti, L., Ferrari, C., Beretta, S., Zappettini, A., Sanchez del Rio, M., Pelliciari, C., Burwitz, V., Ferreira, I., and Bavdaz, M., "BEaTriX: the Beam Expander Testing X-Ray facility for testing ATHENA's SPO modules: progress in the realization," in [*Optics for EUV, X-Ray, and Gamma-Ray Astronomy IX*], *Society of Photo-Optical Instrumentation Engineers (SPIE) Conference Series* **11119**, 111190N (Sept. 2019).

[5] Valsecchi, G., Bianucci, G., Marioni, F., Vernani, D., Zocchi, F. E., Korhonen, T., Pasanen, M., Pareschi, G., Ferreira, I., Bavdaz, M., and Wille, E., "Integration facility for the ATHENA X-Ray Telescope," in [*Optics for EUV, X-Ray, and Gamma-Ray Astronomy IX*], *Society of Photo-Optical Instrumentation Engineers (SPIE) Conference Series* **11119**, 111190M (Sept. 2019).

[6] Guainazzi, M., Bavdaz, M., Burwitz, V., and et al., "ATHENA Mirror Calibration Plan." ESA-ATHENA-ESTEC-SCI-PL-0001.

[7] Burwitz, V., Bradshaw, M., Eder, J., Breunig, E., Ayre, M., Bavdaz, M., and Ferreira, I., "Design of a new long beam x-ray test facility for ATHENA," in [*Society of Photo-Optical Instrumentation Engineers (SPIE) Conference Series*], *Society of Photo-Optical Instrumentation Engineers (SPIE) Conference Series* **11444**, 114444L (Dec. 2020).

[8] Pareschi, G., Moretti, A., Salmaso, B., Sironi, G., Tagliaferri, G., Uslenghi, M., Fiorini, M., Attinà, P., Bressan, R., Marchiori, G., Tordi, M., Marioni, F., Valsecchi, G., and Zocchi, F., "A vertical facility based on raster scan configuration for the x-ray scientific calibrations of the ATHENA optics," in [*International Conference on Space Optics — ICSO 2018*], *Society of Photo-Optical Instrumentation Engineers (SPIE) Conference Series* **11180**, 1118025 (July 2019).

[9] Moretti, A., Pareschi, G., Uslenghi, M., Tordi, M., Bressan, R., Valsecchi, G., Zocchi, F., Attina, P., Amisano, F., Sironi, G., Salmaso, B., Basso, S., Tagliaferri, G., Spiga, D., La Palombara, N., Fiorini, M., Dury, F., Marioni, F., Parissenti, G., Parodi, G., Wille, E., Corradi, P., Bavdaz, M., and Ferreira, I., "VERT-X: VERTical X-ray raster-scan facility for ATHENA calibration. The concept design.," in [*Optics for EUV, X-Ray, and Gamma-Ray Astronomy IX*], *Society of Photo-Optical Instrumentation Engineers (SPIE) Conference Series* **11119**, 111190O (Sept. 2019).

[10] Willingale, R., Pareschi, G., Christensen, F., and den Herder, J.-W., "The Hot and Energetic Universe: The Optical Design of the Athena+ Mirror," *arXiv e-prints* , arXiv:1307.1709 (July 2013).

[11] Biasi, R., Pescoller, D., and Rampini, F., "MicroCLINE: an innovative tiltmeter concept and its application the ALMA-EU antennas' dynamic metrology," in [*Ground-based and Airborne Telescopes III*], Stepp, L. M., Gilmozzi, R., and Hall, H. J., eds., *Society of Photo-Optical Instrumentation Engineers (SPIE) Conference Series* **7733**, 77333N (July 2010).

[12] Willingale, R., "Stray x-ray flux in the Athena Mirror," in [*Optics for EUV, X-Ray, and Gamma-Ray Astronomy IX*], *Society of Photo-Optical Instrumentation Engineers (SPIE) Conference Series* **11119**, 111190Q (Sept. 2019).